



8-1-2003

## The shape parameter of liposomes and DNA-lipid complexes determined by viscometry utilizing small sample volumes

Yan Sun

*Dalian Institute of Chemical Physics Chinese Academy of Sciences*

X. Li

*Dalian Institute of Chemical Physics Chinese Academy of Sciences*

Nejat Düzgüneş

*University of the Pacific Arthur A. Dugoni School of Dentistry, nduzgunes@pacific.edu*

Y. Takaoka

*Tokyo Denki University*

S. Ohi

*Tokyo Denki University*

*See next page for additional authors*

Follow this and additional works at: <https://scholarlycommons.pacific.edu/dugoni-facarticles>

 Part of the [Dentistry Commons](#)

---

### Recommended Citation

Sun, Y., Li, X., Düzgüneş, N., Takaoka, Y., Ohi, S., & Hirota, S. (2003). The shape parameter of liposomes and DNA-lipid complexes determined by viscometry utilizing small sample volumes. *Biophysical Journal*, 85(2), 1223–1232. DOI: [10.1016/S0006-3495\(03\)74558-5](https://doi.org/10.1016/S0006-3495(03)74558-5)  
<https://scholarlycommons.pacific.edu/dugoni-facarticles/593>

This Article is brought to you for free and open access by the All Faculty Scholarship at Scholarly Commons. It has been accepted for inclusion in All Dugoni School of Dentistry Faculty Articles by an authorized administrator of Scholarly Commons. For more information, please contact [mgibney@pacific.edu](mailto:mgibney@pacific.edu).

---

**Authors**

Yan Sun, X. Li, Nejat Düzgüneş, Y. Takaoka, S. Ohi, and S. Hirota

# The Shape Parameter of Liposomes and DNA-Lipid Complexes Determined by Viscometry Utilizing Small Sample Volumes

Y. Sun,\* X. Li,\* N. Düzgüneş,<sup>†</sup> Y. Takaoka,<sup>‡</sup> S. Ohi,<sup>‡</sup> and S. Hirota\*<sup>†‡</sup>

\*Dalian Institute of Chemical Physics, Chinese Academy of Science, Dalian, China; <sup>†</sup>Department of Microbiology, School of Dentistry, University of the Pacific, San Francisco, California USA; and <sup>‡</sup>School of Engineering, Tokyo Denki University, Tokyo, Japan

**ABSTRACT** A minicapillary viscometer utilizing <0.5 ml of sample at a volume fraction of <0.1% is described. The calculated  $a/b$  of DPPC/DPPG multilamellar liposome was 1.14 as prolate ellipsoids and  $a/b$  of dioleoylpropyltrimethyl ammonium methylsulfate-DNA complex at a charge ratio of 4:1 (+/-) was 3.7 as prolate ellipsoids or 4.9 as oblate ellipsoids. The deviation of shape from perfect sphere is thus expressed quantitatively in more than two significant figures. In these measurement, the necessary amount of DNA is <0.5 mg.

## INTRODUCTION

Cationic liposome-DNA complexes (“lipoplexes”) are being utilized as gene delivery vectors both for research and in gene therapy applications (Felgner et al., 1987; Düzgüneş and Felgner, 1993; Düzgüneş et al., 2002; Gao and Huang, 1995; Lasic and Templeton, 1996; Clark and Hersh, 1999; Pedrosa de Lima et al., 2001). The mechanisms of gene delivery by lipoplexes are not well understood and are being investigated. One of the factors that affect gene delivery is the final macromolecular shape of the complexes (Sternberg, 1998; Felgner et al., 1987; Gershon et al., 1993). A capillary viscometer is employed for determining the molecular weight and shape parameter of polymers and their molecular interactions, structure formation in solutions of polymers, as well as for more general specification of liquids (Tanford, 1961). Although viscometry is potentially an excellent tool for quality control of liposomes and lipoplexes, it has seldom been used in this field, most likely because it requires a large amount of sample.

A viscometer which uses a small sample volume (<0.5 ml) would be necessary for studying liposomes containing expensive ingredients. Viscometry using small samples is necessary especially for lipoplexes, because the materials are usually quite expensive. To obtain flow times longer than 100 s for 0.5 ml to flow down a capillary of 20 cm long, the inner diameter of the capillary needs to be <0.5 mm. To measure the intrinsic viscosity of a dilute aqueous solution of DNA, the precision of flow times, in terms of the coefficient of variation (CV), needs to be <0.3%. When the temperature of a thermostat is controlled within  $\pm 0.01^\circ\text{C}$ , two significant figures of the value of the specific viscosity ought to be obtained, with volume fraction <0.02. The reproducibility of the measurements of the flow time through an upper reservoir of 0.5 ml, expressed by standard deviation, is

required to be <0.3 s (0.3%, in terms of CV) to test the viscosity of lipoplexes.

Here we describe an automated minicapillary, viscometer and derive equations for its use in the measurement of the shape parameter of cationic liposome-DNA complexes.

## MATERIALS AND METHODS

### D-glucose aqueous solution

Reagent grade D-glucose was dissolved in double-distilled water. A stock solution of 5.0% (w/v) was diluted to 1.0, 2.0, 3.0, and 4.0% with double-distilled water.

### DPPC/DPPG MLV suspension

Dipalmitoylphosphatidylcholine (DPPC) and dipalmitoylphosphatidylglycerol (DPPG) were mixed at a 9:1 molar ratio in chloroform (total lipid: 0.885 g) and were rotary evaporated to dryness and the dried film was dispersed in 10 ml 10 mM Tris-HCl buffer, pH 8.0. The suspension was sonicated for 2 min in a bath type sonicator and extruded through a 800-nm pore-diameter polytephthalate membrane. This stock solution was diluted to obtain suspensions of  $\phi = 0$  (buffer), 0.0531, 0.0708, and 0.0885 (stock).

### DNA-DOTAP complex suspension

DNA from salmon sperm, sonicated to 80-bp pieces, was complexed with *n*-[1-(2,3-dioleoyloxy)propyl]-*n,n,n* trimethylammonium methylsulfate (DOTAP, FW 698.55) at a molar ratio of 4:1 (+/-) in 10 mM Tris-HCl buffer (pH 7.4).

### Lipoplex preparation by flow impinger

An excess cationic lipid, 2.28 mN DOTAP in 10 mM Tris-HCl buffer (pH 8.0) and an equal volume of 0.57 mN DNA solution in 10 mM Tris-HCl buffer (pH 8.0) were mixed at a charge ratio of 4:1 (+/-), using a flow impinger (Fig. 1). One syringe was filled with a DNA solution and the other with the lipid suspension. Both liquids were injected into the flow impinger at the same volume velocity and impinged in the T-tube 1 at an angle of  $180^\circ$ . The rapid stream created turbulence in chamber 1 and was mixed uniformly. The mixture went into the second T-tube. Thus, three successive impinging and mixing steps made the colloid chemical properties of the complex uniform and the sample was released from the exit into a reservoir. When the volume velocity at each of the above syringes,  $V$ , was 1 ml/s, the maximum shearing rate in the arm of T-tubes, with 0.13-cm inner diameter,  $\gamma' = 4V/\pi r^3$ , is 4000 ( $\text{s}^{-1}$ ) and the Reynolds number in the chamber, with

Submitted December 7, 2002, and accepted for publication March 7, 2003.

Address reprint requests to S. Hirota, 6-6-18 Higashikaigan-Minami, Chigasaki, 253-0054 Japan. Tel.: 81-467-85-8471; Fax: 81-467-57-5080; E-mail: sadaohiro@aol.com.

© 2003 by the Biophysical Society

0006-3495/03/08/1223/10 \$2.00

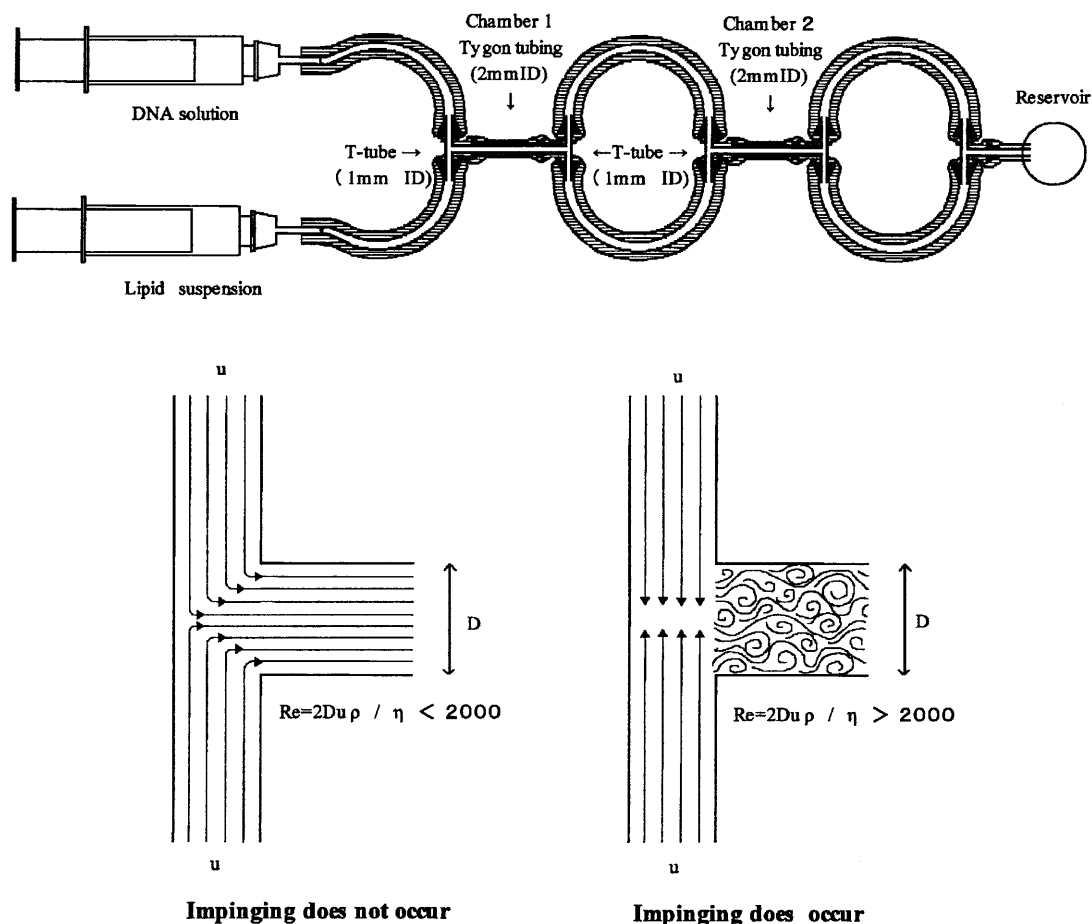


FIGURE 1 Flow impinger. Two syringes are connected to a T-tube, which is connected to two other T-tube units. One syringe is filled with DNA solution and another with lipid suspension. The two pistons are pressed at the same speed. The two liquids impinge at a same velocity at an angle of  $180^\circ$ . Thus, homogeneous mixing of the two liquids is attained. Two pistons are pressed at a same speed. When the Reynolds number ( $Re$ ) is  $<2000$ , impinging does not occur. Even in that case, turbulence of the flow occurs in chambers after the T-tubes and homogeneous mixing of the two liquids is attained.

$D = 0.2$  cm inner diameter,  $Re = DV\rho/\eta\pi^2$ , was 5000 (Hirota et al., 1999). If  $V$  was controlled in the range between 0.5 and 2.0 ml/s, satisfactory mixing and homogenizing was attained without any danger of DNA strand breakage (Bensimon, 1995). The transit time of each liquid through the flow impinger was 0.8 s at  $V = 0.5$  ml/s and 0.2 s at  $V = 2$  ml/s.

The formula weight of the complex was 3124.2 per charge of DNA and its density was 1.001. The final concentration in the stock solution was 0.75 mN of the base unit. Volume fraction of the lipoplex in the stock was  $\phi = 0.001172$ . The stock is diluted to  $\phi = 0$  (buffer), 0.000703, 0.000937, and 0.001171 (stock).

### Minicapillary viscometer

A capillary viscometer with a capillary, an inner diameter of 0.05 cm and 2.0 cm long, and two upper reservoirs, each with an inner volume 0.2 ml, was made of borosilicate glass containing 12–13%  $B_2O_3$  whose softening temperature is  $>718^\circ\text{C}$ . In its upright position, the lower end of the upper reservoir is 3 cm higher than the lower reservoir, which has an inner volume of 1 ml. Both of the upper reservoirs have orifices with 0.1-cm inner diameter (Fig. 2).

### Cannon-Fenske capillary viscometer

A Cannon-Fenske capillary viscometer was purchased from Cole-Palmer International, Vernon Hills, IL (P98934-51). The capillary has an inner

diameter of 0.1 cm and was 20 cm long. The total volume of the upper reservoirs is 7 ml (3 ml + 4 ml) and that of the lower reservoir 15 ml.

### Viscosity measurements

Viscosity measurements by the Cannon-Fenske capillary viscometer were carried out in the standard manner. For measurements by the minicapillary viscometer, the following times were recorded:  $t_{10}$ , for the suspending medium to flow down through the first reservoir from  $a$  to  $b$ ;  $t_{20}$  through the second reservoir from  $b$  to  $c$ ;  $t_{30}$  the total time from  $a$  to  $c$ ;  $t_1$  for the sample to flow through the first reservoir;  $t_2$  for the sample to go through the second reservoir; and the total time,  $t_3$ , for flow through the reservoir from  $a$  to  $c$ . Then,

$$\eta_{\text{rel}} = t_1/t_{10} = t_2/t_{20} = t_3/t_{30} \quad (\text{Newtonian flow}), \quad (1)$$

$$\eta_{\text{rel}} = t_1/t_{10} < t_2/t_{20} \quad (\text{plastic flow, or orientation of particles to the direction of the flow}),$$

$$\eta_{\text{rel}} = t_1/t_{10} > t_2/t_{20} \quad (\text{dilatant flow}).$$

If the liquid is Newtonian, the second and the third terms of Eq. 1 give the same value (within a relative error of 1%). If the two terms are not equal, the liquid is non-Newtonian. In the case of Newtonian flow, the specific viscosity,  $\eta_{\text{sp}}$ , is

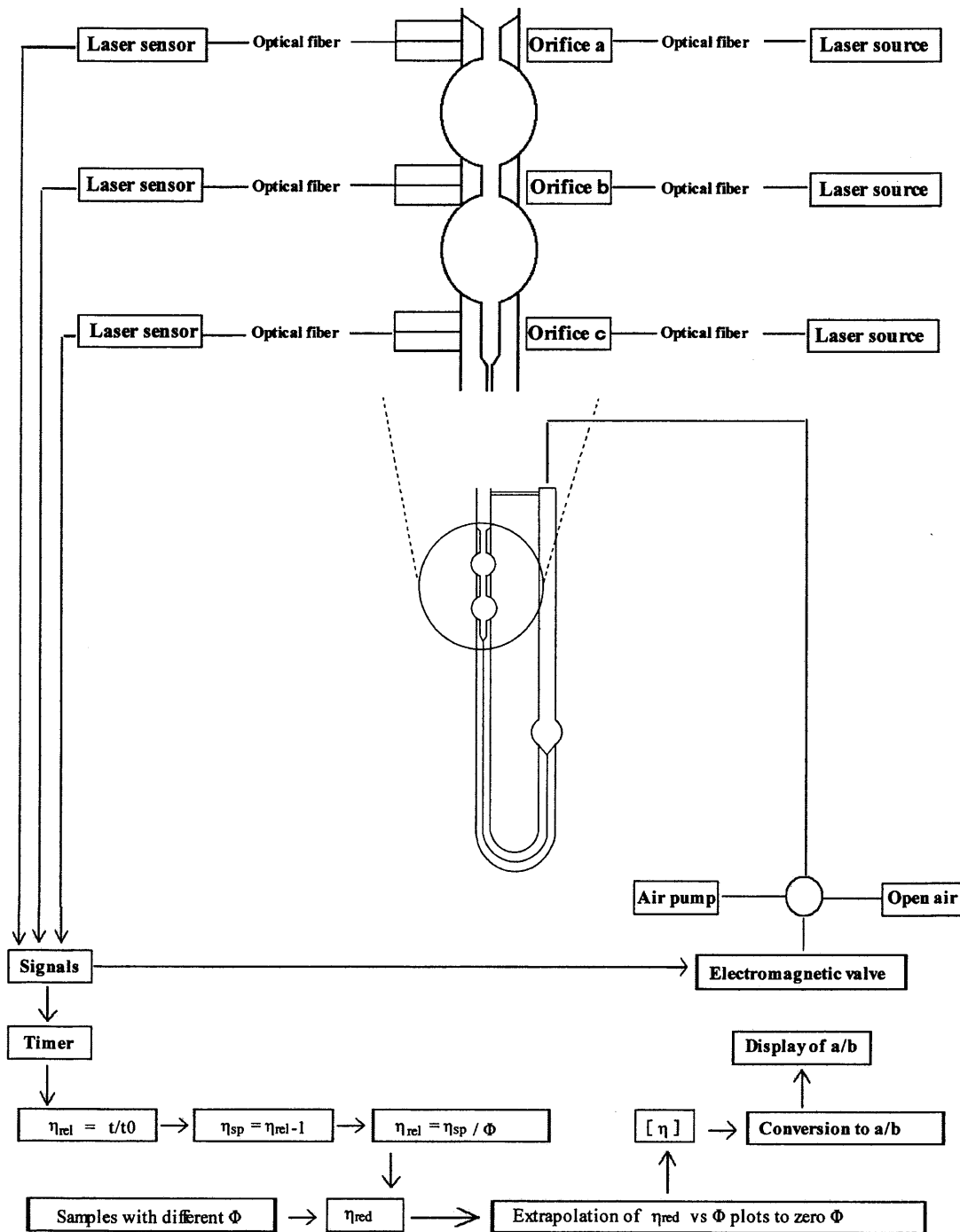


FIGURE 2 Automatic capillary viscometer.

$$\eta_{sp} = \eta_{rel} - 1.$$

When the difference between  $t_1/t_{10}$  and  $t_2/t_{20}$  was within 1%, the values are averaged for the calculation of  $\eta_{sp}$ . Such a slight shear dependence can be neglected and the sample can be regarded as a Newtonian fluid.

When the difference between the values of  $t_1/t_{10}$  and  $t_2/t_{20}$  was  $>1\%$ , the flow time measurements were repeated by tilting the capillary, reducing the head difference until the relative viscosity difference became  $<1\%$ . Shear dependence of the viscosity was thus reduced. Without any effects of orientation, plasticity, or dilatancy, both values became the same in a dilute suspension. When the difference between the values of  $[\eta]$  (below) for  $a \rightarrow b$ ,

$b \rightarrow c$ , and  $a \rightarrow c$  were within 5%, the three were averaged. Simha (1940) calculated the axial ratio assuming that the Brownian motion makes the direction of particle axis isotropic. This condition is attained when the shear effect diminishes under conditions of low flow velocity.

### Determination of nondimensional intrinsic viscosity

Nondimensional intrinsic viscosity  $[\eta]$  was defined by Eq. 4 (below). As there is very little inner aqueous phase in lipoplexes,  $\phi$  could be regarded to

be  $\phi_{\text{net}}$ . Then, the reduced viscosity,  $\eta_{\text{red}} = \eta_{\text{sp}}/\phi_{\text{net}}$ , was plotted against  $\phi_{\text{net}}$ . The  $\phi_{\text{net}}$  was calculated from the amount of DNA and lipids in the sample divided by the density of the particle,  $\rho(\text{g/ml})$ . The density of lipoplexes was assumed to be  $\rho = 1$  in this study. According to the Huggins equation, the plot is on a straight line in the low  $\eta_{\text{red}}$  region. When the obtained plot was not on a straight line, a least-squares line to the plot was drawn and extrapolated to  $\phi_{\text{net}} = 0$ . The intercept on the ordinate provided the nondimensional intrinsic viscosity (e.g., Fig. 3).

### Determination of $a/b$

Simha (1940) extended the Einstein viscosity equation for a suspension of spherical particles to that of ellipsoidal particles as

$$\eta = \eta_0(1 + \nu\phi) \quad (\text{Simha equation}),$$

where  $\eta$  is the viscosity of the suspension,  $\eta_0$  the viscosity of the suspending medium,  $\nu$  a constant, and  $\phi$  the volume fraction of suspended particles. He related  $\nu$  to the axial ratio  $J = a/b$ , where  $a$  is a longer semidiameter and  $b$  the shorter semidiameter, as

$$\nu = [J^2/15(\ln 2J - 1.5)] + [J^2/5(\ln 2J - 0.5) + (14/15)] \quad (\text{for prolate ellipsoid}),$$

$$\nu = (16/15)(J/\tan^{-1}J) \quad (\text{for oblate ellipsoid}).$$

Although the Simha equation holds irrespective of particle size and fractionation is not necessary, it holds only in the range of  $a/b > 50$ . This range is too large for lipoplexes used for gene delivery. For studying and quality control of lipoplex shape, a definite value of  $a/b$  much smaller than 50 is required. However, Simha gave only the results of calculated numerical values for  $a/b$  in this region (Mehl et al., 1940). It is difficult to use the numerical table in a simple inexpensive integrated circuit chip for a computerization of the measurement.

The Simha equation can be expressed in the form

$$\nu\phi = (\eta/\eta_0) - 1 = \eta_{\text{sp}}, \quad (2)$$

where  $\eta_{\text{sp}}$  is the specific viscosity, and

$$\nu = \eta_{\text{sp}}/\phi = \eta_{\text{red}}. \quad (3)$$

Let us call  $\eta_{\text{red}}$  the nondimensional reduced viscosity. The Simha equation holds only when the particles are nonattracting. With realistic particles this condition is attained in an infinite dilution; then,

$$\nu = \lim_{\phi \rightarrow 0} \eta_{\text{red}} = [\eta]. \quad (4)$$

Let us call  $[\eta]$  the nondimensional intrinsic viscosity. Note that Simha factor,  $\nu$ , is nothing but nondimensional intrinsic viscosity.

We have obtained simple equations relating the nondimensional intrinsic viscosity,  $[\eta]$ , to axial ratios of ellipsoids in the range of  $1 < a/b < 100$  by a Newtonian approximation to Simha's results,

$$[\eta] = 0.057(a/b)^2 + 0.61a/b + 1.83 \quad (\text{for prolate ellipsoid}), \quad (5)$$

$$[\eta] = 0.001(a/b)^2 + 0.59a/b + 1.90 \quad (\text{for oblate ellipsoid}). \quad (6)$$

An average shape parameter of the DNA-lipid complex, expressed by the axial ratio,  $a/b$ , of an ellipsoid is given by viscometry using Eqs. 5 and 6. It is postulated that the complexation is complete and that there are no free DNA molecules in the suspension. Any size fractionation of particles and determination of each size is not necessary, because the Simha equation holds irrespective of particle size at infinite dilution. The relationship between the nondimensional intrinsic viscosity and the axial ratio of prolate and oblate ellipsoid is given in Table 1 and compared to Simha's results (Fig. 4). The nondimensional intrinsic viscosity,  $[\eta]$ , thus obtained is converted to the axial ratio,  $a/b$ , by Eqs. 5 and 6.

## RESULTS

### Reproducibility

In a preliminary experiment, the reproducibility of the flow time measurement was far from the requirement that the standard deviation be  $< 0.3$  s. The reproducibility was especially poor when the sample was an aqueous suspension of lipoplexes. The reason for the poor reproducibility was thought to be the formation of a water-repellent lipid monomolecular layer on the inner surface of the capillary. Even the adherence of an invisible air bubble has a significant effect on the flow time, because the flow time is inversely proportional to the fourth power of the capillary diameter. Trials to remove the water-repellent film with detergent or organic solvents were not successful. Heating the capillary  $> 500^\circ\text{C}$  for 20 min in a furnace resulted in the removal of the

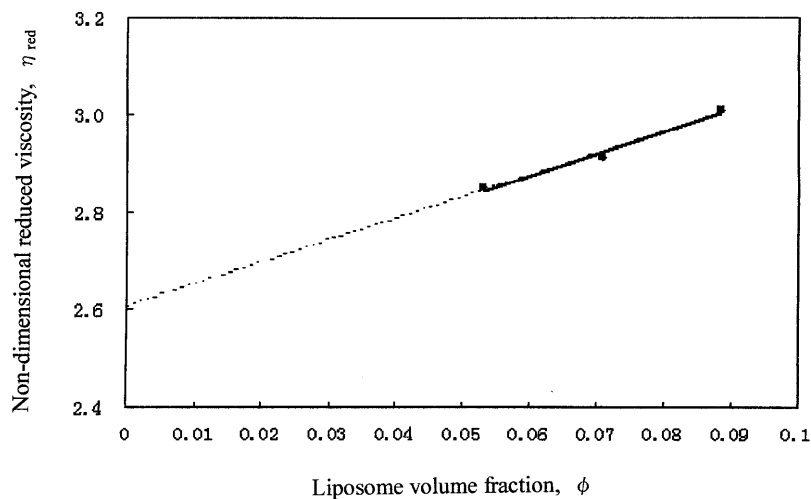


FIGURE 3 Determination of the nondimensional intrinsic viscosity of the DPPC/DPPG multilamellar vesicles suspension.

**TABLE 1**  $[\eta]$  versus  $a/b$ , and  $a/b$  versus  $[\eta]$  relationship

| $[\eta]$ | $(a/b)_{\text{prolate}}$ by Eq. 5 | $(a/b)_{\text{oblate}}$ by Eq. 6 | $a/b$ | $[\eta]_{\text{prolate}}$ by Eq. 5 | $[\eta]_{\text{oblate}}$ by Eq. 6 | $[\eta]_{\text{prolate}}$ by Simha | $[\eta]_{\text{oblate}}$ by Simha |
|----------|-----------------------------------|----------------------------------|-------|------------------------------------|-----------------------------------|------------------------------------|-----------------------------------|
| 2.5      | 1                                 | 1                                | 1     | 2.5                                | 2.5                               | 2.5                                | 2.5                               |
| 2.6      | 1.14                              | 1.16                             | 1.1   | 2.57                               | 2.55                              |                                    |                                   |
| 2.7      | 1.28                              | 1.32                             | 1.2   | 2.64                               | 2.61                              |                                    |                                   |
| 2.8      | 1.40                              | 1.49                             | 1.3   | 2.72                               | 2.67                              |                                    |                                   |
| 2.9      | 1.54                              | 1.65                             | 1.4   | 2.79                               | 2.73                              |                                    |                                   |
| 3.0      | 1.65                              | 1.81                             | 1.5   | 2.88                               | 2.79                              | 2.63                               | 2.62                              |
| 3.2      | 1.90                              | 2.13                             | 1.6   | 2.95                               | 2.65                              |                                    |                                   |
| 3.4      | 2.13                              | 2.45                             | 1.8   | 3.12                               | 2.96                              |                                    |                                   |
| 3.6      | 2.36                              | 2.77                             | 2     | 3.28                               | 3.1                               | 2.91                               | 2.85                              |
| 3.8      | 2.60                              | 3.11                             | 3     | 4.17                               | 3.7                               | 3.68                               | 3.43                              |
| 4.0      | 2.82                              | 3.4                              | 4     | 5.18                               | 4.3                               | 4.66                               | 4.06                              |
| 4.2      | 3.04                              | 3.65                             | 5     | 6.31                               | 4.9                               | 5.81                               | 4.71                              |
| 4.4      | 3.20                              | 4                                | 6     | 7.54                               | 5.5                               | 7.01                               | 5.36                              |
| 4.6      | 3.30                              | 4.3                              | 7     | 8.89                               | 6.1                               |                                    |                                   |
| 4.8      | 3.50                              | 4.6                              | 8     | 10.36                              | 7                                 | 10.1                               | 6.7                               |
| 5.0      | 3.70                              | 5                                | 9     | 11.9                               | 7.3                               |                                    |                                   |
| 5.5      | 4.2                               | 5.7                              | 10    | 13.6                               | 7.9                               | 13.63                              | 8.04                              |
| 6.0      | 4.8                               | 6.5                              | 11    | 15.5                               | 9                                 |                                    |                                   |
| 6.5      | 5.2                               | 7.2                              | 12    | 17.4                               | 9.7                               | 17.76                              | 9.39                              |
| 7.0      | 5.5                               | 8                                | 13    | 18.8                               | 10.4                              |                                    |                                   |
| 7.5      | 5.9                               | 8.7                              | 14    | 21.6                               | 11.1                              |                                    |                                   |
| 8.0      | 6.3                               | 9.6                              | 15    | 23.9                               | 11.8                              | 24.8                               | 11.42                             |
| 8.5      | 6.7                               | 10.3                             | 16    | 26.3                               | 12.5                              |                                    |                                   |
| 9.0      | 7.1                               | 11                               | 17    | 28.6                               | 13.3                              |                                    |                                   |
| 9.5      | 7.4                               | 11.7                             | 18    | 31.4                               | 14                                |                                    |                                   |
| 10       | 7.7                               | 12.4                             | 19    | 34.1                               | 14.7                              |                                    |                                   |
| 11       | 8.3                               | 13.8                             | 20    | 36.9                               | 14.9                              | 38.6                               | 14.8                              |
| 12       | 9                                 | 15.3                             | 21    | 39.9                               | 16.3                              |                                    |                                   |
| 13       | 9.6                               | 16.8                             | 22    | 41.5                               | 17                                |                                    |                                   |
| 14       | 10.2                              | 18.2                             | 23    | 42.9                               | 17.8                              |                                    |                                   |
| 15       | 10.7                              | 19.5                             | 24    | 49.4                               | 18.6                              |                                    |                                   |
| 20       | 13                                | 26.8                             | 25    | 52.8                               | 19.4                              | 55.2                               | 18.9                              |
| 25       | 15                                | 33                               | 30    | 71.5                               | 22.5                              | 74.5                               | 21.6                              |
| 30       | 17.3                              | 40                               | 40    | 120                                | 31.3                              | 120.8                              | 28.3                              |
| 40       | 21                                | 50                               | 50    | 173                                | 41.9                              | 176.5                              | 35                                |
| 50       | 24                                | 65                               | 70    | 324                                | 60                                | 242                                | 41.7                              |
|          |                                   |                                  |       |                                    |                                   | 400.1                              | 55.1                              |
| 100      | 35                                | 134                              | 100   | 633                                | 71                                | 593                                | 68.6                              |
| 150      | 45                                | 190                              | 150   | 1376                               | 110                               | 1222                               | 102.3                             |
| 200      | 57                                | 240                              | 200   | 2404                               | 160                               | 2051                               | 136.2                             |
| 250      | 61                                | 290                              | 250   | 3718                               | 210                               |                                    |                                   |
| 300      | 67                                | 325                              | 300   | 5315                               | 270                               | 4560                               | 220                               |
| 350      | 76                                | 360                              | 350   | 7199                               | 330                               | 6026                               | 260                               |
| 400      | 80                                | 400                              | 400   | 9366                               | 400                               | 7674                               | 300                               |
| 500      | 90                                | 465                              | 500   | 14557                              | 550                               | 11481                              | 380                               |
| 1000     | 126                               | 750                              | 1000  | 57612                              | 1590                              | 40271                              | 760                               |

Comparison of Hirota's to Simha's results for prolate ellipsoid,  $[\eta]_{\text{prolate}} = 0.057(a/b)^2 + 0.61(a/b) + 1.83$  (Eq. 5); and for oblate ellipsoid,  $[\eta]_{\text{oblate}} = 0.001(a/b)^2 + 0.59(a/b) + 1.9$  (Eq. 6).

water-repellent film from the inner surface of the capillary. A microcapillary viscometer was produced, with heat-resistant glass which is stiff enough at 550°C for 20 min. After the heating of the viscometer in the furnace, the reproducibility of the flow time data was improved remarkably, even with measurements of suspensions containing cationic lipids. When the flow time increased and the CV exceeded 0.3%, the viscometer was rinsed and heated in the furnace. Then the original flow time data were obtained again. It was confirmed that repeated heating does not result in any changes in the inner diameter of the capillary.

### D-glucose solution

The flow times and viscosity data of aqueous D-glucose are shown in Tables 2 and 3. Data obtained by the conventional Cannon-Fenske capillary viscometer and by the minicapillary viscometer were in good agreement.

### DPPC-DPPG MLV suspension

The flow times and viscosity data are shown in Table 4. The nondimensional reduced viscosities are plotted against the

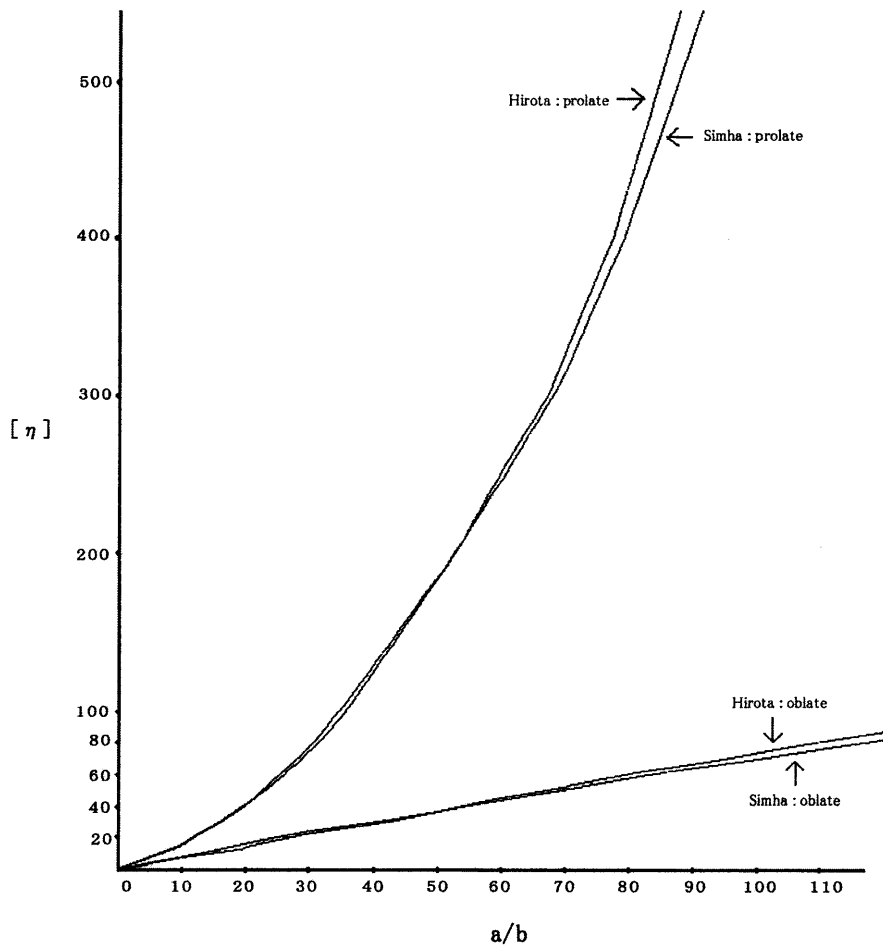


FIGURE 4 Relationship of nondimensional intrinsic viscosity,  $[\eta]$ , to the axial ratio,  $a/b$ , of an ellipsoid.

TABLE 2 Viscosity of aqueous D-glucose solution at 30°C, by Cannon-Fenske viscometer

| No.   | Weight fraction |                   | $t$ (s)           |        |        |        |        | AV     | SD     | CV     | $\eta_{rel}$ |
|-------|-----------------|-------------------|-------------------|--------|--------|--------|--------|--------|--------|--------|--------------|
|       |                 |                   | 1                 | 2      | 3      | 4      | 5      |        |        |        |              |
| 0     |                 | $a \rightarrow b$ | 118.38            | 118.51 | 118.48 |        |        | 118.46 | 0.0681 | 0.0006 |              |
| Water |                 | $b \rightarrow c$ | 184.84            | 184.89 | 185.04 |        |        | 184.92 | 0.1041 | 0.0006 |              |
|       |                 | $a \rightarrow c$ | 303.22            | 303.4  | 303.52 | 303.45 |        | 303.4  | 0.1282 | 0.0004 |              |
|       | 1               | 0.01              | $a \rightarrow b$ | 123.57 | 123.3  | 123.35 | 123.26 |        | 123.37 | 0.1383 | 0.0011       |
|       | 0.01            | $b \rightarrow c$ | 192.91            | 193.12 | 192.93 | 193.01 |        | 192.99 | 0.0954 | 0.0005 | 1.0436       |
|       | 0.01            | $a \rightarrow c$ | 316.48            | 316.42 | 316.28 | 316.27 |        | 316.36 | 0.104  | 0.0003 | 1.0427       |
| 2     | 0.02            | $a \rightarrow b$ | 128.49            | 128.39 | 128.26 | 128.75 |        | 128.47 | 0.2076 | 0.0016 | 1.0846       |
|       | 0.02            | $b \rightarrow c$ | 200.66            | 201.09 | 201.47 | 200.9  |        | 201.03 | 0.3421 | 0.0017 | 1.0871       |
|       | 0.02            | $a \rightarrow c$ | 329.15            | 329.48 | 329.73 | 329.65 | 329.71 | 329.54 | 0.2412 | 0.0007 | 1.0862       |
| 3     | 0.03            | $a \rightarrow b$ | 133.93            | 134.44 | 134.62 | 134.3  | 134.43 | 134.34 | 0.2579 | 0.0019 | 1.1341       |
|       | 0.03            | $b \rightarrow c$ | 209.49            | 210.11 |        | 210.49 | 210.32 | 210.1  | 0.4369 | 0.0021 | 1.1362       |
|       | 0.03            | $a \rightarrow c$ | 343.42            | 344.55 |        | 344.79 | 344.75 | 344.38 | 0.6469 | 0.0019 | 1.1351       |
| 4     | 0.04            | $a \rightarrow b$ | 146.17            | 145.83 | 145.8  | 145.97 | 144.9  | 145.73 | 0.4886 | 0.0034 | 1.2303       |
|       | 0.04            | $b \rightarrow c$ | 228.8             | 228.47 | 228.64 |        | 228.63 | 228.64 | 0.1348 | 0.0006 | 1.2364       |
|       | 0.04            | $a \rightarrow c$ | 374.97            | 374.3  | 374.44 |        | 373.53 | 374.31 | 0.5947 | 0.0016 | 1.2337       |
| 5     | 0.05            | $a \rightarrow b$ | 146.3             | 146.46 | 146.16 |        |        | 146.31 | 0.1501 | 0.001  | 1.2351       |
|       | 0.05            | $b \rightarrow c$ | 229.11            | 229.05 | 228.91 |        |        | 229.02 | 0.1026 | 0.0004 | 1.2385       |
|       | 0.05            | $a \rightarrow c$ | 375.41            | 375.51 | 375.07 |        |        | 375.33 | 0.2307 | 0.0006 | 1.2371       |

Data is  $t_{10}$ ,  $t_{20}$ ; (s) is flow time of water, in seconds;  $t_1$ ,  $t_2$  is the flow time of aqueous D-glucose solution from  $a \rightarrow b$ ,  $a \rightarrow c$ , and  $b \rightarrow c$ ; the relative viscosity is  $\eta_{rel} = t_1/t_{10}$ ,  $t_2/t_{20}$  through the same reservoir, e.g.,  $a \rightarrow b$ ; the weight fraction is the weight of solute/weight of solution; AV is the average; SD is the standard deviation; and CV is the coefficient of variation. Temperature is  $30.00 \pm 0.01^\circ\text{C}$ .



**TABLE 3 Viscosity of aqueous D-glucose solution at 30°C, by minicapillary viscometer**

| Sample | Weight fraction |                     | <i>t</i> (s) |        |        |        | AV     | SD     | CV     | $\eta_{rel}$ |
|--------|-----------------|---------------------|--------------|--------|--------|--------|--------|--------|--------|--------------|
|        |                 |                     | 1            | 2      | 3      | 4      |        |        |        |              |
| 0      |                 | <i>a</i> → <i>b</i> | 187.43       |        | 187.42 | 187.14 | 187.33 | 0.1646 | 0.0009 |              |
| Water  |                 | <i>b</i> → <i>c</i> | 316.09       |        | 315.07 | 314.49 | 315.22 | 0.81   | 0.0026 |              |
|        |                 | <i>a</i> → <i>c</i> | 503.52       | 502.33 | 502.49 | 501.63 | 502.49 | 0.7802 | 0.0016 |              |
| 1      | 0.01            | <i>a</i> → <i>b</i> | 194.79       | 194.89 | 194.74 |        | 194.81 | 0.0764 | 0.0004 | 1.0399       |
|        | 0.01            | <i>b</i> → <i>c</i> | 327.45       | 327.35 | 327.37 |        | 327.39 | 0.0529 | 0.0002 | 1.0386       |
|        | 0.01            | <i>a</i> → <i>c</i> | 522.24       | 522.24 | 522.11 | 522.27 | 522.22 | 0.0714 | 0.0001 | 1.0392       |
| 2      | 0.02            | <i>a</i> → <i>b</i> | 204.28       | 203.58 | 203.72 | 204.17 | 203.94 | 0.3398 | 0.0017 | 1.0887       |
|        | 0.02            | <i>b</i> → <i>c</i> | 339.53       | 339.66 | 340.38 | 339.74 | 339.83 | 0.3784 | 0.0011 | 1.0781       |
|        | 0.02            | <i>a</i> → <i>c</i> | 543.81       | 543.24 | 544.1  | 543.91 | 543.77 | 0.3701 | 0.0007 | 1.0821       |
| 3      | 0.03            | <i>a</i> → <i>b</i> | 213.23       | 214.17 | 213.67 | 213.2  | 213.57 | 0.4555 | 0.0021 | 1.1401       |
|        | 0.03            | <i>b</i> → <i>c</i> | 354.84       | 354.18 | 354.45 | 356.05 | 354.88 | 0.8257 | 0.0023 | 1.1258       |
|        | 0.03            | <i>a</i> → <i>c</i> | 568.07       | 568.35 | 568.12 | 569.25 | 568.45 | 0.5487 | 0.001  | 1.1313       |
| 4      | 0.04            | <i>a</i> → <i>b</i> | 222.36       | 221.18 | 221.99 |        | 221.84 | 0.6035 | 0.0027 | 1.1842       |
|        | 0.04            | <i>b</i> → <i>c</i> | 370.78       | 371.41 | 370.02 |        | 370.74 | 0.696  | 0.0019 | 1.1761       |
|        | 0.04            | <i>a</i> → <i>c</i> | 593.14       | 592.59 | 592.01 |        | 592.58 | 0.5651 | 0.001  | 1.1793       |
| 5      | 0.05            | <i>a</i> → <i>b</i> | 235.83       | 236.04 | 235.51 | 236    | 235.85 | 0.2412 | 0.001  | 1.259        |
|        | 0.05            | <i>b</i> → <i>c</i> | 392.86       | 392.03 | 392.15 | 391.24 | 392.07 | 0.6636 | 0.0017 | 1.2438       |
|        | 0.05            | <i>a</i> → <i>c</i> | 628.69       | 628.07 | 627.66 | 627.24 | 627.92 | 0.6179 | 0.001  | 1.2496       |

Data is  $t_{10}$ ,  $t_{20}$ ; (s) is the flow time of water, in seconds;  $t_1$ ,  $t_2$  is the flow time of sample solutions, *a*→*c* and *b*→*c*; the relative viscosity is  $\eta_{rel} = t_1/t_{10}$ ,  $t_2/t_{20}$  through the same reservoir, e.g., *a*→*b*; the weight fraction is the weight of solute/weight of solution; AV is the average; SD is the standard deviation; and CV is the coefficient of variation. Temperature is  $30.00 \pm 0.01^\circ\text{C}$ .

volume fractions (Fig. 3). From Fig. 3, the nondimensional intrinsic viscosity was determined to be 2.6. The corresponding axial ratios were 1.14 for a prolate ellipsoid and 1.16 for an oblate ellipsoid. Electron microscopy of negatively stained samples revealed prolate ellipsoids (Fig. 5). The coefficient of variation of the flow time (CV) seldom exceeded 0.1%, and the data were very reproducible.

**DNA-DOTAP complex**

The flow times and viscosity data are shown in Table 5. The nondimensional intrinsic viscosity was determined to be 4.99 from Fig. 6, and corresponds to axial ratios of 3.7 for a prolate ellipsoid and 4.9 for an oblate ellipsoid. These data are obtained with a DNA sample as small as 0.5 mg.

**TABLE 4 Viscosity of multilamellar DPPC/DPPG vesicles suspension**

| Sample     | $\phi$    |                     | Flow time, s        |                     |        |        | AV     | SD     | CV     | $\eta_{rel}$ | $\eta_{sp}$ | $\eta_{red}$ |
|------------|-----------|---------------------|---------------------|---------------------|--------|--------|--------|--------|--------|--------------|-------------|--------------|
|            |           |                     | 1                   | 2                   | 3      |        |        |        |        |              |             |              |
| Buffer     | 0         | <i>a</i> → <i>b</i> | 98.45               | 98.58               | 98.83  | 98.62  | 0.1931 | 0.0020 |        |              |             |              |
|            | 0         | <i>a</i> → <i>c</i> | 251.80              | 251.90              | 252.00 | 251.89 | 0.0971 | 0.0004 |        |              |             |              |
|            | 0         | <i>b</i> → <i>c</i> | 153.30              | 153.30              | 153.10 | 153.27 | 0.1097 | 0.0007 |        |              |             |              |
| 1          | 0.053     | <i>a</i> → <i>b</i> | 113.10              | 113.00              | 113.20 | 113.08 | 0.0643 | 0.0006 | 1.1466 | 0.1466       | 2.7606      |              |
|            | 0.053     | <i>a</i> → <i>c</i> | 290.30              | 290.10              | 290.10 | 290.16 | 0.1069 | 0.0004 | 1.1520 | 0.1520       | 2.8618      |              |
| 2          | 0.053     | <i>b</i> → <i>c</i> | 177.20              | 177.00              | 177.00 | 177.09 | 0.1266 | 0.0007 | 1.1554 | 0.1554       | 2.9268      |              |
|            | 0.071     | <i>a</i> → <i>b</i> | 118.20              | 118.00              | 118.50 | 118.22 | 0.2654 | 0.0022 | 1.1987 | 0.1987       | 2.8066      |              |
|            | 0.071     | <i>a</i> → <i>c</i> | 304.00              | 304.10              | 304.20 | 304.10 | 0.0814 | 0.0003 | 1.2073 | 0.2073       | 2.9280      |              |
| 3          | 0.071     | <i>b</i> → <i>c</i> | 185.80              | 186.20              | 185.70 | 185.89 | 0.2635 | 0.0014 | 1.2128 | 0.2128       | 3.0061      |              |
|            | 0.089     | <i>a</i> → <i>b</i> | 124.40              | 123.80              | 124.00 | 124.15 | 0.2906 | 0.0023 | 1.2589 | 0.2589       | 2.9251      |              |
|            | 0.089     | <i>a</i> → <i>c</i> | 319.70              | 318.80              | 319.10 | 319.23 | 0.4107 | 0.0013 | 1.2673 | 0.2673       | 3.0207      |              |
|            | 0.089     | <i>b</i> → <i>c</i> | 195.30              | 195.00              | 195.10 | 195.08 | 0.1630 | 0.0008 | 1.2728 | 0.2728       | 3.0823      |              |
|            | $\phi$    | <i>a</i> → <i>b</i> | <i>a</i> → <i>c</i> | <i>b</i> → <i>c</i> | AV     |        |        |        |        |              |             |              |
| 1          | 0.053     | 2.761               | 2.862               | 2.927               | 2.85   |        |        |        |        |              |             |              |
| 2          | 0.071     | 2.806               | 2.928               | 3.006               | 2.91   |        |        |        |        |              |             |              |
| 3          | 0.089     | 2.925               | 3.021               | 3.082               | 3.01   |        |        |        |        |              |             |              |
| [ $\eta$ ] | $\phi$ →0 | 2.507               | 2.619               | 2.694               | 2.60   |        |        |        |        |              |             |              |

Sample is 0.885 g PC/PG (9/1), dispersed in 10 ml/10 mM Tris-HCl buffer, pH 8.0, prepared by the Bangham method; and the volume fraction of stock suspension is  $\phi = 0.0885$ . Temperature is  $40.00 \pm 0.01^\circ\text{C}$ . Obtained nondimensional intrinsic viscosity of 2.6 corresponds to *a/b* of 1.14 (prolate) and 1.16 (oblate).

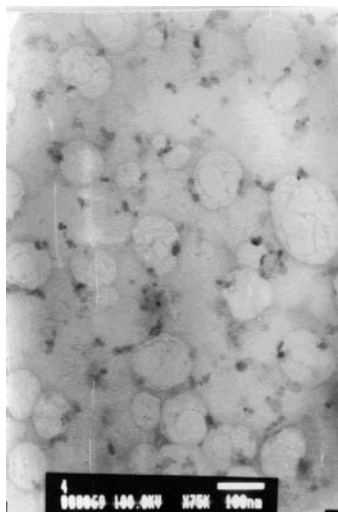


FIGURE 5 Negative stain electron micrograph of DPPC/DPPG multilamellar vesicles.

## DISCUSSION

As small unilamellar vesicles are almost a perfect sphere,  $[\eta]$  is  $\sim 2.5$  (data not shown). The Simha equation reduces to the Einstein equation for dilute suspension of nonattracting spherical particles,

$$\eta = \eta_0(1 + 2.5\phi) \quad (\text{Einstein equation}).$$

If  $[\eta]$  values  $> 2.5$  are observed, it may indicate aggregation of the particles. Multilamellar vesicles and large unilamellar vesicles are not always spherical. The shape factor in these cases is seldom important. However, the shape factor is one of the most important characteristics of lipoplexes or other DNA complexes, because it is one of the determinants of their transfection efficiency (Sternberg, 1998; Felgner et al.,

1987; Gershon et al., 1993). The shape of liposomes and lipoplexes is also speculated to affect their in vivo distribution after intravenous, subcutaneous, or intratumoral delivery. The shape of lipoplex has been determined by electron or atomic force microscopy. These techniques, however, give only local information without an overall average value. For quality control in a large-scale production, a quantitative average value is necessary. Small-angle x-ray scattering, low-angle light scattering, quasi-elastic laser scattering, and photon-correlation spectroscopy give overall information on the shape of particles. Instrumentation for these techniques may be too expensive and the necessary expertise may not be readily available to adopt them in process control units in production plants. Similarly, a small pharmacy unit in a clinic may not be able to adopt these tests for clinical trials. Viscometry may turn out to be a more suitable method for this purpose.

According to the Mark-Houwink equation (Mark, 1938; Houwink, 1941) expressed nondimensionally,

$$\ln[\eta] = \ln 2.5 + \alpha \ln M. \quad (7)$$

When the shape parameter,  $\alpha$ , equals 0 the particles are rigid spheres, while  $\alpha = 2$  means that the particles are straight filaments. Although Eq. 7 gives information on the shape of particles in suspension, determination of  $\alpha$  requires many measurements of the dependence of  $[\eta]$  on  $M$ . For this purpose, fractionation of the sample suspension and determination of  $\phi$  for each fraction are needed, requiring much labor and large quantities of the sample.

The shape of liposomes and DNA-lipid complexes are also characterized by the axial ratio of an ellipsoid using Eqs. 5 and 6. As Eqs. 5 and 6 hold irrespective of particle size, time-consuming fractionations and determinations of  $\phi$  for each fraction are not necessary.

The formation of a lipoplex is thought to proceed via the following steps (Oberle et al., 2000):

TABLE 5 Viscosity of DNA-DOTAP complex suspension

| $\phi$   |                   | 1      | 2      | 3      | AV     | SD     | CV     | $\eta_{rel}$ | $\eta_{sp}$ | $\eta_{red}$ |
|----------|-------------------|--------|--------|--------|--------|--------|--------|--------------|-------------|--------------|
|          | $a \rightarrow b$ | 170.61 | 170.37 | 170.51 | 170.5  | 0.1206 | 0.0007 |              |             |              |
|          | $b \rightarrow c$ | 151.77 | 151.78 | 151.51 | 151.69 | 0.1531 | 0.001  |              |             |              |
|          | $a \rightarrow c$ | 322.38 | 322.15 | 322.02 | 322.18 | 0.1823 | 0.0006 |              |             |              |
| 0.000703 | $a \rightarrow b$ | 171.23 | 171.09 | 171.09 | 171.14 | 0.0808 | 0.0005 | 1.0038       | 0.0038      | 5.3399       |
| 0.000703 | $b \rightarrow c$ | 152.83 | 151.84 | 151.95 | 152.21 | 0.5426 | 0.0036 | 1.0034       | 0.0034      | 4.8767       |
| 0.000703 | $a \rightarrow c$ | 324.06 | 322.93 | 323.04 | 323.34 | 0.6231 | 0.0019 | 1.0036       | 0.0036      | 5.1218       |
| 0.000937 | $a \rightarrow b$ | 171.62 | 170.95 | 171.81 | 171.46 | 0.4518 | 0.0026 | 1.0057       | 0.0057      | 6.0283       |
| 0.000937 | $b \rightarrow c$ | 152.55 | 152.23 | 152.07 | 152.28 | 0.2444 | 0.0016 | 1.0039       | 0.0039      | 4.1968       |
| 0.000937 | $a \rightarrow c$ | 324.17 | 323.18 | 323.88 | 323.74 | 0.509  | 0.0016 | 1.0048       | 0.0048      | 5.166        |
| 0.001172 | $a \rightarrow b$ | 171.48 | 171.95 | 171.36 | 171.6  | 0.3118 | 0.0018 | 1.0065       | 0.0065      | 5.5068       |
| 0.001172 | $b \rightarrow c$ | 152.81 | 152.03 | 152.81 | 152.55 | 0.4503 | 0.003  | 1.0057       | 0.0057      | 4.8579       |
| 0.001172 | $a \rightarrow c$ | 324.29 | 323.98 | 324.17 | 324.15 | 0.1563 | 0.0005 | 1.0061       | 0.0061      | 5.2013       |

Sample is DNA from salmon sperm, sonicated to 100 bp, complexed with *n*-[1-(2,3-dioleoyloxy)propyl]-*n,n,n*-trimethylammonium methylsulfate (DOTAP, FW 774.2) in a molar ratio of 4:1 (+/-) dissolved in Tris-HCl buffer at pH 7.4. The complex has a FW of 3425.8 and a density of 1.001. Final concentration in the stock solution is 0.75 mN of the base unit. Volume fraction of the lipoplex in the stock is  $\phi = 0.001172$ . The stock is diluted to  $\phi = 0.000703, 0.000937$ . Temperature is  $30.00 \pm 0.001^\circ\text{C}$ .

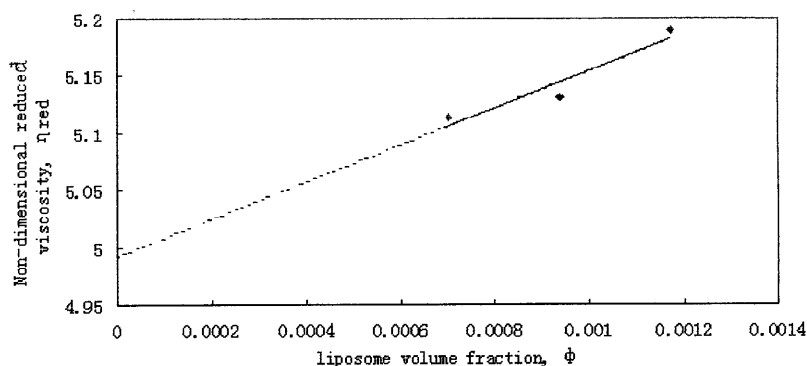


FIGURE 6 Determination of nondimensional intrinsic viscosity of the DOTAP-DNA (4:1 molar ratio) complex's suspension.

DNA + excess cationic lipid vesicles  $\rightarrow$  complex 1 (rapid electrostatic process, within 1 s).

Segregation of complex 1  $\rightarrow$  complex 2 (slow process by dispersion force within 1 h).

Fusion of vesicles and collapse of the lipid film to form a multilamellar sheath around DNA (maturation)  $\rightarrow$  lipoplex in equilibrium  $\rightarrow$  complex 3 (very slow process in hours or days at room temperature).

The time it takes for the solution to pass through the flow-impinger is less than 1 s. Although this is enough for formation of complex 1, it is too short for completing the formation of complex 2. If the aggregates are dispersed in the solution with excess cationic lipid vesicles in some flow condition for a few hours, all the particles would become the final complex 3. The shape of the lipoplex is thought to depend not only on the size of DNA, but also on the flow condition during the maturation. However, the relation between the flow conditions and the rheological shape parameter of the final lipoplex is not clear at this time. A quantitative study to follow the time course of lipoplex maturation will be possible viscometrically using Eqs. 5 and 6.

## CONCLUSION

A simple technique for the determination of the shape of liposomes and cationic liposome-DNA complexes is proposed using a minicapillary viscometer that requires a minimal amount of sample, in combination with a new type of viscometric measurement. The nondimensional intrinsic viscosity  $[\eta]$  is related to the axial ratio,  $a/b$ , of an ellipsoid, and is applicable to low axial ratios (in the range of  $1 < a/b < 100$ ) by  $[\eta] = 0.057(a/b)^2 + 0.61a/b + 1.83$  (for prolate ellipsoid; Eq. 5), and  $[\eta] = 0.001(a/b)^2 + 0.59a/b + 1.90$  (for oblate ellipsoid; Eq. 6).

The combination of the minicapillary viscometer and the new viscometric measurements is practical in the study of DNA-lipid complexes, and possibly other particles including liposomes and bioactive polymers. Almost perfect sphericity of DPPC-DPPG liposomes was ex-

pressed by the axial ratios,  $a/b$ , of 1.14 (prolate) and 1.16 (oblate), whereas DNA-DOTAP lipoplexes have ratios of 3.7 (prolate) and 4.9 (oblate). The deviation of shape from perfect sphere is thus expressed quantitatively in more than two significant figures. The required amount of DNA is as small as 0.5 mg.

We thank Prof. J. Cohen, Dr. K. Konopka and researchers at the University of the Pacific, Prof. F. Szoka at the University of California, San Francisco, and the late Dr. D. D. Lasic, for their helpful discussions and suggestions.

## REFERENCES

- Bensimon, D. 1995. Stretching DNA with a receding meniscus: experiments and models. *Phys. Rev. Lett.* 74:4754–4760.
- Clark, P. R., and E. M. Hersh. 1999. Cationic lipid-mediated gene transfer: current concepts. *Curr. Opin. Mol. Ther.* 1:158–176.
- Düzgünes, N., and P. L. Felgner. 1993. Intracellular delivery of nucleic acids and transcription factors by cationic liposomes. *Methods Enzymol.* 221:303–306.
- Düzgünes, N., S. Simões, P. Pires, and M. C. Pedroso de Lima. 2002. Gene delivery by cationic liposome-DNA complexes. In *Polymeric Biomaterials*. S. Dumitriu, editor. Marcel Dekker, New York. pp. 943–958.
- Felgner, P. L., T. R. Gadek, M. Holm, R. Roman, H. W. Chan, M. Wenz, J. P. Northrop, G. M. Ringold, and M. Danielsen. 1987. Lipofection: a highly efficient, lipid-mediated DNA-transfection procedure. *Proc. Natl. Acad. Sci. USA.* 84:7413–7417.
- Gao, X., and L. Huang. 1995. Cationic liposome-mediated gene transfer. *Gene Ther.* 2:710–722.
- Gershon, H. R., R. Ghirlando, S. B. Guttman, and A. Minsky. 1993. Mode of formation and structural features of DNA-cationic liposome complexes used for transfection. *Biochemistry.* 32:7143–7151.
- Hirota, S., C. Tros de Ilarduya, L. Barron, and F. Szoka. 1999. Simple mixing device to reproducibly prepare cationic lipid-DNA complexes (lipoplexes). *Biotechniques.* 27:286–289.
- Houwink, R. J. 1941. *Prakt. Chem.* 157:15. Cited in *Physical Chemistry of Macromolecules*. 1961. C. Tanford, author. John Wiley and Sons, New York. pp.391–456.
- Lasic, D. D., and N. S. Templeton. 1996. Liposomes in gene therapy. *Adv. Drug Deliv. Rev.* 20:221–266.
- Mark, H. 1938. *Der feste Koerper*. Hirzel, Leipzig. 103. Cited in *Physical Chemistry of Macromolecules*. 1961. C. Tanford, author. John Wiley and Sons, New York. pp.391–456.

- Mehl, J. W., J. L. Oncley, and R. Simha. 1940. Viscosity and the shape of protein molecules. *Science*. 92:132–133.
- Oberle, V., U. Bakowsky, I. S. Zuhorn, and D. Hoekstra. 2000. Lipoplex formation under equilibrium conditions reveals a three-steps mechanism. *Biophys. J.* 79:1447–1454.
- Pedroso de Lima, M. C., S. Simões, P. Pires, H. Faneca, and N. Düzgüneş. 2001. Cationic lipid-DNA complexes in gene delivery: from biophysics to biological applications. *Adv. Drug Deliv. Rev.* 47:277–294.
- Simha, R. 1940. The influence of Brownian movement on the viscosity of solutions. *J. Phys. Chem.* 44:25–34.
- Sternberg, B. 1998. Ultrastructural morphology of cationic liposome-DNA complexes for gene therapy. *In Medical Applications of Liposomes*. D. D. Lasic, editor. pp.395–427.
- Tanford, C. 1961. *Physical Chemistry of Macromolecules*. John Wiley and Sons, New York. pp.317–451.